CHEMBIOCHEM

DOI: 10.1002/cbic.200700387

Effect of Cu^{II} on the Complex between Kanamycin A and the Bacterial Ribosomal A Site

Duccio Balenci,[a] Francesca Bernardi,[a] Luciano Cellai,[b] Nicola D'Amelio,[a] Elena Gaggelli,[a] Nicola Gaggelli,[a] Elena Molteni,[a] and Gianni Valensin*[a]

The solution structure of kanamycin A interacting with a ribosomal A-site fragment was solved by transferred-NOE techniques and found to agree with the structure of the complex observed in the crystal. Despite the fast exchange conditions found for the interaction, the bound form was identified by NOESY spectroscopy. At 600 MHz, NOE effects are only observed for the RNA-associated antibiotic. Dissociation constants were measured by NMR spectroscopy for two sites of interaction ($K_{d1} = 150 \pm 40$ μM; $K_{d2} = 360 \pm 50$ μM). Furthermore, the effects of the Cu^{II} ion on the antibiotic, on the RNA fragment that mimics the bacterial ribosomal A site, and on the complex formed between these two entities were analyzed. The study led to the proposal of a model that localizes the copper ion within the kanamycin–RNA complex.

Introduction

Aminoglycosides, a large family of clinically important antibiotics, are polycationic water-soluble molecules that consist of two or more amino sugars joined through glycosidic linkages to a 2-deoxystreptamine ring.[1–3] The 2-deoxystreptamine ring is substituted at the 4- and 5-positions in the neomycin class and at the 4- and 6-positions in the kanamycin and gentamycin classes.[2] Positively charged at physiological pH values, aminoglycosides can bind to the negatively charged RNA backbone. The high flexibility of these molecules facilitates their accommodation within internal loops, bulges, and cavities of the complex architecture of RNA through noncovalent shape-specific rather than sequence-specific interactions.[4]

Aminoglycosides exert their therapeutic properties by binding to the 16S subunit of ribosomal RNA at an asymmetrical internal loop, which is an essential component of the codon–anticodon recognition site (A site): This interaction disturbs the decoding process and induces misreading of the genetic code.[5,6] The decoding A site is composed of nucleotides 1400–1410 and 1490–1500, and contains two universally conserved adenine residues at positions 1492 and 1493. The asymmetrical internal loop is closed by the Watson–Crick base pair C1407–G1494 and the noncanonical base pairs U1406–U1495 and A1408–A1493. Decoding occurs through the interaction of the A site with the backbone of the codon–anticodon helix. During decoding, the A site changes its conformation from an "off" (A1492 and A1493 are folded in the shallow groove of the A site) to an "on" mode (A1492 and A1493 bulge out fully from the A site).[7–9] This conformational change is necessary to enable A1492 and A1493 to interact specifically with the first two of the three base pairs formed by the cognate codon–anticodon interaction.[7] It also provokes the transition of the ribosome from an open to a closed form stabilized by contacts involving the cognate tRNA and the ribosome.[9,10]

The binding of aminoglycosides at a pocket created by the base pair A1408–A1493 and the single bulged adenine residue A1492 induces a structural rearrangement and locks the A site in the "on" conformation. In this way, the translocation of the tRNA–mRNA complex is inhibited and fidelity of translation disrupted.[1,11–14] The ribosome loses its ability to discriminate between correct and incorrect tRNA, and incorrect amino acids are incorporated during protein synthesis. As a result, nonfunctional, misfolded proteins are synthesized, which leads ultimately to bacterial cell death.[9,10,15]

Although aminoglycosides are a very important group of chemotherapeutics in clinical use, they cause irreversible damage to the auditory system[16–19] and have also been reported to induce other severe toxic effects, such as nephrotoxicity.[20,21] The ability of aminoglycosides to form stable complexes with copper(II) at physiological pH owing to the occurrence of several amine and hydroxy donors led to a hypothesis that the toxicities associated with the antibiotics can be caused by an oxidative mechanism.[22] Not only is the aminoglycoside protonation state (which can be affected by the presence of Cu^{II}) altered upon its recognition by RNA,[23] but the oxidation of guanine, the nucleobase that displays the lowest oxidation potential,[24] has been shown to proceed through a one- rather than a two-electron mechanism. This mechanism might account for the observed cleavage of target RNA or DNA by copper aminoglycosides.[25,26] Moreover, even if aminoglycosides themselves are redox inactive,[27,28] the resulting copper complexes are capable of converting hydrogen per-

[a] D. Balenci, Dr. F. Bernardi, Dr. N. D'Amelio, Prof. E. Gaggelli, Dr. N. Gaggelli, Dr. E. Molteni, Prof. G. Valensin
Department of Chemistry, University of Siena
Via A. Moro, 53100 Siena (Italy)
Fax: (+39) 0577-234254
E-mail: valensin@unisi.it

[b] Prof. L. Cellai
Istituto di Cristallografia, CNR
Area della Ricerca di Roma 1, 00016 Monterotondo Stazione (Italy)

oxide into water and dioxygen with the production of reactive oxygen species.[27,29–32]

Although the intracellular concentration of free copper ions is kept extremely low by specific chaperone proteins,[33] extracellular copper ions in human blood serum may be coordinated by several ligands,[34,35] and the concentration of copper ions can be relevant to some pathological conditions, such as cancer and inflammation.[36] It is not unlikely that some copper ions are transferred to aminoglycosides during clinical treatment.[37]

The Cu^{II} complex of the aminoglycoside kanamycin A (KanA) has been investigated extensively.[29,38] The formation of ternary complexes of copper(II), kanamycin A, and nucleic acids has been reported.[39] It was also found that copper(II) complexes of imino and amino sugars oxidize 2-deoxyguanosine (dG) efficiently in the presence of hydrogen peroxide and thus convert dG into its 8-oxo derivative.[40,41] The relevance of these studies is supported by the evidence that Cu^{II} complexes are highly efficient in cleaving DNA and RNA.[26,30,42–44] This effect might have an additional role in inhibiting protein synthesis and thus enhancing antibiotic activity,[30,45] although this issue has been a matter of debate.[46]

In this study we tried to elucidate the structural aspects of the interaction between kanamycin A and an RNA fragment of 23 nucleotides containing the decoding A site of bacterial ribosome in the presence and in the absence of the Cu^{II} ion. First, the solution structure of the bound antibiotic was solved by transferred-NOE techniques. The structure obtained is in good agreement with the X-ray crystal structure of the complex of KanA with the rRNA A site;[47] such a finding is not trivial in the light of previously reported differences between NMR-derived and crystallographic structures of aminoglycosides complexed with an RNA A-site oligonucleotide.[48] Paramagnetic effects were then interpreted to localize the copper ion in the antibiotic–RNA complex. The structural model might help explain the metal-catalyzed RNA-cleavage activity of aminoglycosides associated with copper.

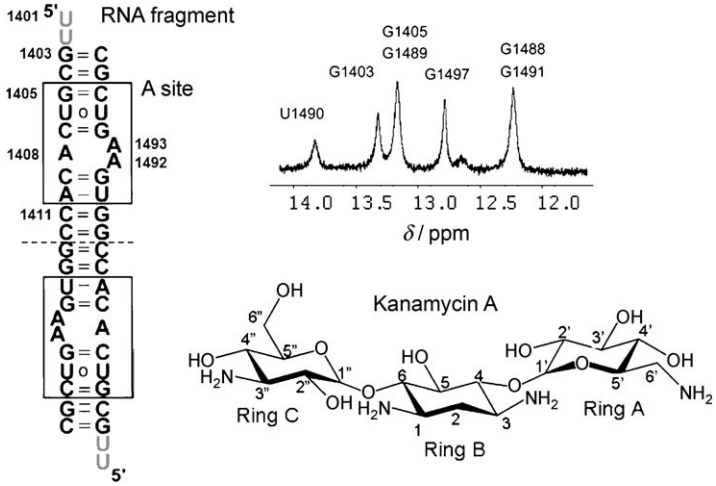

Figure 1. ^{1}H NMR spectrum of an RNA fragment that mimics the ribosomal A site. The spectrum was recorded at a concentration of 0.62 mM in H_2O and phosphate buffer (20 mM) at pH 6.5 and $T = 298$ K. The structures of the RNA fragment and kanamycin A are also shown.

Table 1. Assignment of the ^{1}H NMR signals [ppm] of RNA (0.36 mM) in H_2O/phosphate buffer (20 mM) in the presence of NaCl (0.1 M) at pH 6.5 and $T = 298$ K.

Nucleotide	6-H/8-H	5-H/2-H	1′-H	NH	NH_2
U1401	7.61	5.67			
U1402	7.82	5.82	5.96		
G1403	7.98		5.67	13.31	
C1404	7.72	5.30	5.38		8.43, 6.58
G1405	7.44		5.67	13.16	
U1406	7.51	5.37	5.04		
C1407	7.90	5.65	5.64		8.19, 6.99
A1408	8.05		5.89		
C1409	7.49	5.30	5.16		8.35, 6.81
A1410	8.07	7.40	5.83		6.11
C1411	7.51	5.13			6.80, 8.23
C1412	7.63	5.37	5.37		6.57, 8.22
G1413	7.41		5.69	12.22	
G1414	7.19		5.68	13.15	
U1415	7.53	5.09	5.12	13.82	
G1416	7.54		5.74	12.22	
A1417	8.15		5.94		
A1418	8.29	8.13	5.99		
G1419	7.35		5.51		
U1420	7.71	5.62	5.18		
C1421	7.77	5.68	5.54		6.76, 7.61
G1422	7.56		5.67	12.77	
C1423	8.00	5.74	5.43		7.02, 8.19

Results and Discussion

Our study was aimed at elucidating the role of the copper(II) ion in the interaction between kanamycin A and an RNA fragment that reproduces the prokariotic A site of the ribosome (Figure 1). To gain a deep understanding of the system, we first investigated the interaction between KanA and the RNA fragment in solution. Having determined the main structural features of the complex and the dissociation constant, we investigated the effect of the presence of copper(II) on the RNA fragment alone, on the antibiotic alone, and on the complex.

Assignment of the signals in the ^{1}H NMR spectrum

The ^{1}H NMR signals observed for the RNA fragment were assigned by 2D TOCSY and 2D NOESY experiments (Table 1). The sample (0.62 mM) was dissolved in H_2O to enable the detection of U and G imino hydrogen atoms, the signals for which are found in the well-resolved region between 15 and 10 ppm. The imino hydrogen atoms of the terminal U1401 and U1402 residues, which are not base paired, are not detectable as a result of exchange with the solvent; for the same reason, the signals for the imino hydrogen atoms of U1406 and U1495, which form a weak noncanonical base pair, are extremely broad.

In the 2D NOESY spectrum, the imino hydrogen atom of U1490 correlates strongly with the 2-H aromatic hydrogen atom of the base-paired adenine residue A1410; the imino hydrogen atoms of guanine nucleotides show a dipolar correlation with the 1′-H atom of their own sugars and with the amino and 5-H hydrogen atoms of the base-paired cytosine residues. The amino groups of guanine and adenine residues are not detected as result of exchange with the solvent. From the amino groups of cytosines, it is possible to assign the 5-H and 6-H hydrogen atoms, which also display a strong cross-peak in the TOCSY spectrum. Finally, as cross-peaks are observed in the NOESY spectrum for 6-H (of cytosine and uracyl) and 8-H (of guanine and adenine) with the 1′-H atom of both their own and the previous sugar, the sugars can be assigned sequentially by following the correlation pathway 6-H/8-H→1′-H→6-H/8-H. The signals for sugar hydrogen atoms other than 1′-H overlap excessively in the 1D and 2D spectra and were not assigned.

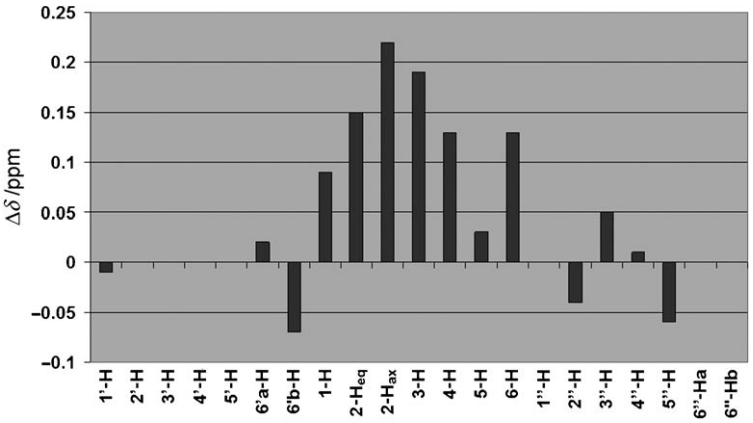

Figure 2. ^{1}H NMR chemical-shift deviations (ppm) observed for kanamycin A upon its interaction with the RNA fragment. Deviations were measured by using a sample of kanamycin A (0.4 mM) in the presence of RNA (KanA/RNA 10:1) in H_2O and phosphate buffer (20 mM) at pH 6.5 and $T = 298$ K.

The results of the assignment of the ^{1}H NMR signals for kanamycin A by TOCSY and COSY 2D experiments at pH 6.5 are in agreement with previous results.[38] A concentration of kanamycin A of 0.4 mM was chosen to minimize aggregation phenomena that arise from intermolecular interactions between protonated amino groups and the electron pairs of ring oxygen atoms. We demonstrated previously[38] that when kanamycin A is dissolved in water, all rings adopt a chair conformation with all substituents in an equatorial position, except the linkages between rings A and B and rings B and C. Moreover, the magnetic nonequivalence of the 6-H atoms in rings A and C suggested the formation of a five-membered ring through a hydrogen bond connecting either the amino group (ring A) or the hydroxy group (ring C) and the oxygen atom of the ring. The complete solution structure was described recently by Asensio et al.[49] Whereas the C ring is in the *syn* Ψ conformation with respect to the B ring (hydrogen atoms bonded to carbon atoms of interconnected rings face one another), the A ring can adopt both *syn* and *anti* Ψ conformations, the latter of which has an occupation of 50% at lower pH values.

Interaction of the RNA fragment with KanA

Addition of the antibiotic to the sample of RNA leads to changes in the chemical shifts observed for atoms over the entire RNA fragment. This observation indicates a significant rearrangement of the macromolecule to harbor the kanamycin molecule. Not all chemical shifts could be measured for kanamycin A under these conditions as a result of extensive broadening of the signals and their overlap with signals from the macromolecule. Instead, the differences in the chemical shifts of all hydrogen atoms were measured for a sample of the antibiotic (0.4 mM) in the presence of a small amount of RNA (in a 10:1 ratio; Figure 2). The largest variations were observed for ring B. The chemical shifts for ring B correlate well with the X-ray crystal structure[47] in the sense that ring B displays more contacts with the RNA. In particular, in the crystallographic structure, five RNA atoms are within 0.3 nm of ring B (all localized around the 2-H atoms); there are only three RNA atoms in such close proximity to the A ring (one of them is near the amino group bonded to 6′-C, and only two so close to the C ring).

By titrating the RNA fragment with the antibiotic up to the addition of 2.5 equivalents, it was possible to evaluate the binding constant of the antibiotic (Figure 3) on the basis of changes in the chemical shift of isolated imino protons. Further addition of kanamycin A results in signal disappearance

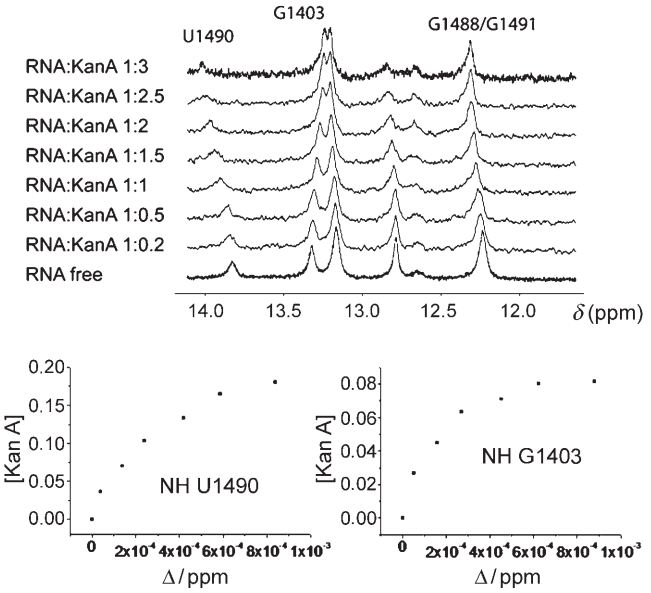

Figure 3. ^{1}H NMR spectra of the RNA fragment (0.62 mM) in H_2O and phosphate buffer (20 mM) at pH 6.5 and $T = 298$ K in the presence of an increasing amount of kanamycin A (up to a KanA/RNA ratio of 3:1). The curves obtained by plotting the concentration of kanamycin A against the observed changes in the chemical-shifts of the clearly identifiable imino hydrogen atoms of U1490 and G1403 are also shown.

and/or overlap, which prevent the measurement of chemical shifts. Different constants were observed for different signals, which confirms the presence of multiple interactions, as found in the X-ray crystal structure.[47] On the basis of the contacts found for different binding modes in the X-ray crystal structure and the observed chemical shifts of the imino hydrogen atoms of G1403 and U1490, we concluded that these residues are associated with the so-called "specific" and "nonspecific" interaction, respectively.[47]

The variation in the chemical shift (Δ) of the hydrogen atoms of RNA is proportional to the molar fraction of the kanamycin A added, which indicates that the aminoglycoside forms a complex that is in fast exchange on the NMR time scale. Standard regression analysis was used to fit the obtained exponential curve by using Equation (1),[50] which can be rearranged to give Equation (2), in which Δ_0 is the limit value of the chemical-shift variation, and K_d is the dissociation constant. [KanA] is given by Equation (3), in which C_{Kan} and C_{RNA} are the analytical concentrations of KanA and RNA (as a monomer).[51]

$$\Delta = \Delta_0 \frac{[\text{KanA}]}{K_d + [\text{KanA}]} \quad (1)$$

$$[\text{KanA}] = \frac{-K_d \Delta}{\Delta - \Delta_0} \quad (2)$$

$$[\text{KanA}] = C_{Kan} - C_{RNA} \frac{\Delta}{\Delta_0} \quad (3)$$

At first we calculated [KanA] values from Equation (3) by using a rough estimate of Δ_0 as the last Δ value in the titration. By fitting the data reported in Figure 3 with Equation (2), a new value of Δ_0 was found, and the process was repeated to the point of convergence. This procedure enabled the estimation of the limiting value for the "specific" (Δ_0) and "aspecific" (Δ_0') sites. To calculate the K_d value of the specific site, the experimental concentration of the antibiotic was corrected by using Equation (4), in which the prime symbol refers to the chemical shifts observed for the competing site U1490, to compensate for the fact that RNA also binds KanA in the aspecific site. An analogous procedure was used to calculate the K_d value of the aspecific site.

$$[\text{KanA}] = C_{Kan} - C_{RNA} \frac{\Delta}{\Delta_0} - C_{RNA} \frac{\Delta\prime}{\Delta'_0} \quad (4)$$

We found K_d values of 150 ± 40 μM and 360 ± 50 μM for specific and nonspecific binding, respectively. Similar values for the specific site ($K_d = 90 \pm 30$ μM) were found by analyzing the variation in the chemical shift of the imino hydrogen atoms of G1491 (the signals of which overlap with those for G1488). The values are larger than those found previously for a similar system ($K_d = 18$ μM).[52]

The stoichiometry of the complex was obtained by using the relationship in Equation (5), in which n is the stoichiometric coefficient assigned to RNA and $\bar{\nu}$ is the molar concentration ratio given by Equation (6).[52]

$$\frac{\bar{\nu}}{C_{RNA}} = \frac{n}{K_d} - \frac{\bar{\nu}}{K_d} \quad (5)$$

$$\bar{\nu} = \frac{C_{RNA}}{C_{Kan}} \frac{\Delta}{\Delta_0 - \Delta} \quad (6)$$

For both specific and nonspecific equilibria, the expected 1:1 stoichiometry was found, which demonstrates the consistency of the approach used.

The variation observed for the equatorial 2-H atom of the B ring of KanA was used to verify independently the dissociation constant found, as the signal for this hydrogen atom can be observed clearly even at high RNA/KanA ratios. When KanA is present in tenfold excess, we can assume a bound molar fraction of 0.1 (that is, all the RNA is bound), and we can estimate the chemical shifts of the bound antibiotic to be shifted with respect to those observed for the free form by ten times the variation observed under our experimental conditions. Complete binding at a KanA/RNA ratio of 10:1 is confirmed by the NOESY spectrum (Figure 4). The intensities of the cross-peaks originating from RNA and from the bound antibiotic are similar; this indicates that all KanA is bound. (The intramolecular cross-peaks of KanA are all due to its RNA-bound fraction; see the section "Structural analysis of the complex"). As we know the limiting value of the variations ($\Delta_0 = \delta_{bound} - \delta_{free}$), it is possible to determine the molar fraction of the bound antibi-

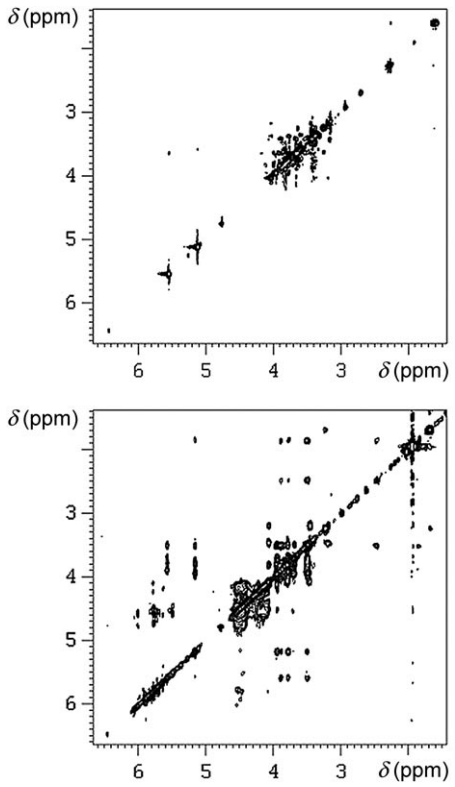

Figure 4. ^{1}H NOESY spectra of kanamycin A (0.40 mM) in H_2O and phosphate buffer (20 mM) at pH 6.5 and $T = 298$ K in the absence of the RNA fragment (left) and in the presence of the RNA fragment in a RNA/KanA ratio of 1:10 (right).

otic, x_{bound}, from the observed chemical shift, Δ, by using the equation $x_{bound} = \Delta/\Delta_0$. Under the experimental conditions of the titration, the value Δ of the equatorial 2-H atom of the B ring at a RNA/KanA ratio of 1:2.5 corresponds to a molar fraction of 0.21. This value is in good agreement with the theoretical molar fraction expected for a complex with the K_d value measured ($x_b = 0.28$) and serves as independent confirmation of the validity of the binding constant, as it was obtained by considering the chemical shifts of the ligand (rather than those of the RNA, on which the fitting was based).

Structural analysis of the complex

For the structural characterization of the bound form of the antibiotic, we exploited the fact that the large size of kanamycin A results in the existence of a range of motions, which make the cross-relaxation rate (and thus the NOE effect) vanish at 600 MHz. In fact, the NOESY spectrum of free kanamycin A showed no correlations outside the diagonal (Figure 4). The addition of 0.1 equivalents of the RNA fragment causes the appearance of intramolecular cross-peaks of kanamycin A as a result of a slower tumbling of the complex. This small amount of RNA does not perturb the spectrum significantly.

NOESY cross-peaks that arise from the interaction serve as a direct probe for the bound conformation. The intensities of these cross-peaks were converted into intramolecular interproton distance restraints (Table 2) to calculate the structure of kanamycin A bound to RNA. As a result of extensive overlap of the proton signals of kanamycin A, several intraring volumes were measured and used as reference intensities for distance calibration. The small chemical-shift changes observed in the presence of 0.1 equivalents of RNA (Figure 2) allowed us to assume that the conformation found in free kanamycin A for rings A and C is maintained (see the section "Assignment of the signals in the ^{1}H NMR spectrum"). A change in conformation would result in large changes in the chemical shifts. Such changes would be observable even when scaled down by the factor of 0.1 that corresponds to the proportion of the bound form present. As for the B ring, the changes in the chemical shifts can be ascribed to the formation of hydrogen bonds between amino/hydroxy groups and RNA moieties (as revealed by the X-ray crystal structure), rather than to a difference in the conformation of the ring with respect to the free form. In fact, the chair conformation found in the free form with all substituents in equatorial positions implies that the intensity of the cross-peak between 4-H/6-H and 2-H_{ax} (0.25 nm apart) should be stronger than the intensity of the cross-peak between 4-H/6-H and 2-H_{eq} (0.37 nm), which is what we found in the presence of RNA. In contrast, in a chair conformation with all substituents in axial positions, the distance between 4-H/6-H and 2-H_{eq} would be 0.38 nm, and the distance between 4-H/6-H and 2-H_{ax} would be 0.43 nm.

We used the distance constraints to construct the pseudo potential energy of the system for structural determination through a simulated annealing procedure in torsional angle space with the program DYANA.[53] The structure obtained was compared with the crystallographic structure[47] of kanamycin A complexed with the same RNA fragment (Figure 5) and found to be quite similar, although two different binding sites were found in the crystal. The two bound conformations are almost superimposable (the root-mean-square deviation is 0.05 nm), and the proton–proton distances used as constraints have the same values in the two complexes within experimental error. The main difference in the structure determined by NMR spectroscopy is a slight reorientation of the C ring. This difference can probably be ascribed to mobility and/or intrinsic errors originating from different NOE build-up rates between coupled protons. As the relative orientation of the three rings is very much dependent on the value of just a few interring-distance constraints, these errors can lead easily to slightly different orientations of the rings. Furthermore, our structure is a weighted average of the two specifically and nonspecifically bound molecules, which, although very similar, probably display different mobility. The *syn* Ψ conformation found for both the A and the C ring with respect to the B ring in the obtained structure indicates that the interaction does not require significant rearrangement. Apparently, the low percentage of the *anti* Ψ conformation found in the free form between the A and the B ring[49] is not determinant in the bound form.

Table 2. Intramolecular proton–proton distances for KanA in the KanA–RNA complex.

Atom 1	Atom 2	*r* (lower limit) [nm]	*r* (upper limit) [nm]
1′-H	4-H	0.24	0.26
1″-H	6-H	0.27	0.31
1″-H	2-H_{ax}	0.43	0.49
1″-H	2-H_{eq}	0.38	0.44
1′-H	2-H_{ax}	0.5	–
1′-H	2-H_{eq}	0.5	–

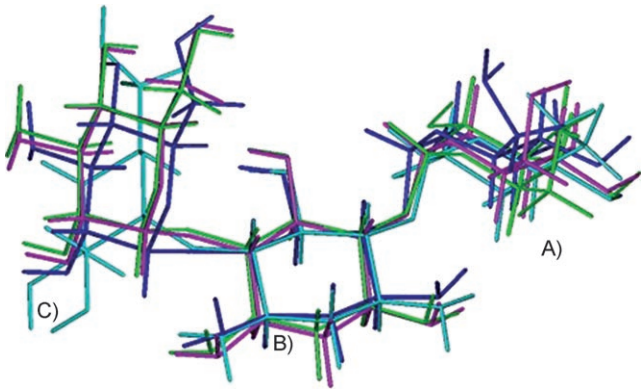

Figure 5. Structures of kanamycin A bound to the RNA fragment. The best NMR experimental structure is depicted in blue, the X-ray crystal structure in cyan. The best DYANA structure after energy minimization with (green) and without (magenta) distance constraints is also shown.

Effect of copper on RNA

The bases of RNA contain many donor atoms, which can provide several good anchoring points for copper(II). We added Cu^{II} to RNA in a Cu^{II}/RNA ratio of 5:1 and investigated their interaction by examining the NMR spectra for line broadening. In the region between 12 and 15 ppm, where the signals of the imino hydrogen atoms of guanine and uracil residues occur, a clear broadening of the peaks for G1488, G1489, and U1490 was observed (Figure 6A). This effect was confirmed by the disappearance of the NOESY cross-peaks of the amino groups of C1411 and C1412, which are base paired to the guanine residues G1488 and G1489 (Figure 6D). However, this region is not the only region affected by copper. We stress that effects on amine groups of G and A residues are not detectable because of the absence of their signals in the NMR spectrum, probably as a result of fast exchange with the solvent.

Most of the signals in the region between 8.8 and 6.4 ppm decrease in intensity upon the addition of Cu^{II} (Figure 6B). The effect on cytosine residues is observed clearly in the TOCSY spectrum, in which a cross-peak between 6-H and 5-H identifies C and U bases unequivocally (Figure 6C). However, the broadening is differential, with C1412 (and to a lesser extent C1404, C1407, and probably U1490) affected more than the other C and U bases. Little can be said about U1406 and U1495 owing to significant signal overlap in this region. The hydrogen atoms 2-H and 8-H of G and A bases are also affected (they can be distinguished from exchangeable protons by comparing the spectrum in D_2O); however, we are unable to give detailed information for such bases as a result of extensive signal overlap and the absence of isolated cross-peaks in the NOESY spectrum. Smaller effects can be detected in the remaining region, which corresponds to the sugar moieties of RNA and the terminal U bases. Finally, ^{31}P NMR spectra show unselective broadening of the phosphate signals (data not shown).

In conclusion, copper(II) ions interact aspecifically with RNA, although the region located around the C1411–G1489 base pair is more affected than others. The binding of Cu^{II} to N1, N3, or N7 of A or G bases cannot be excluded owing to the absence of isolated proton signals for nearby atoms.

Effect of copper on KanA

The effect of copper(II) on KanA has been studied extensively at different pH values.[29,38] Their coordination is dependent on the pH value, but a common feature of the complexes is the involvement of the nitrogen atom of the C ring. Complexation with copper at higher pH values also involves the A ring of

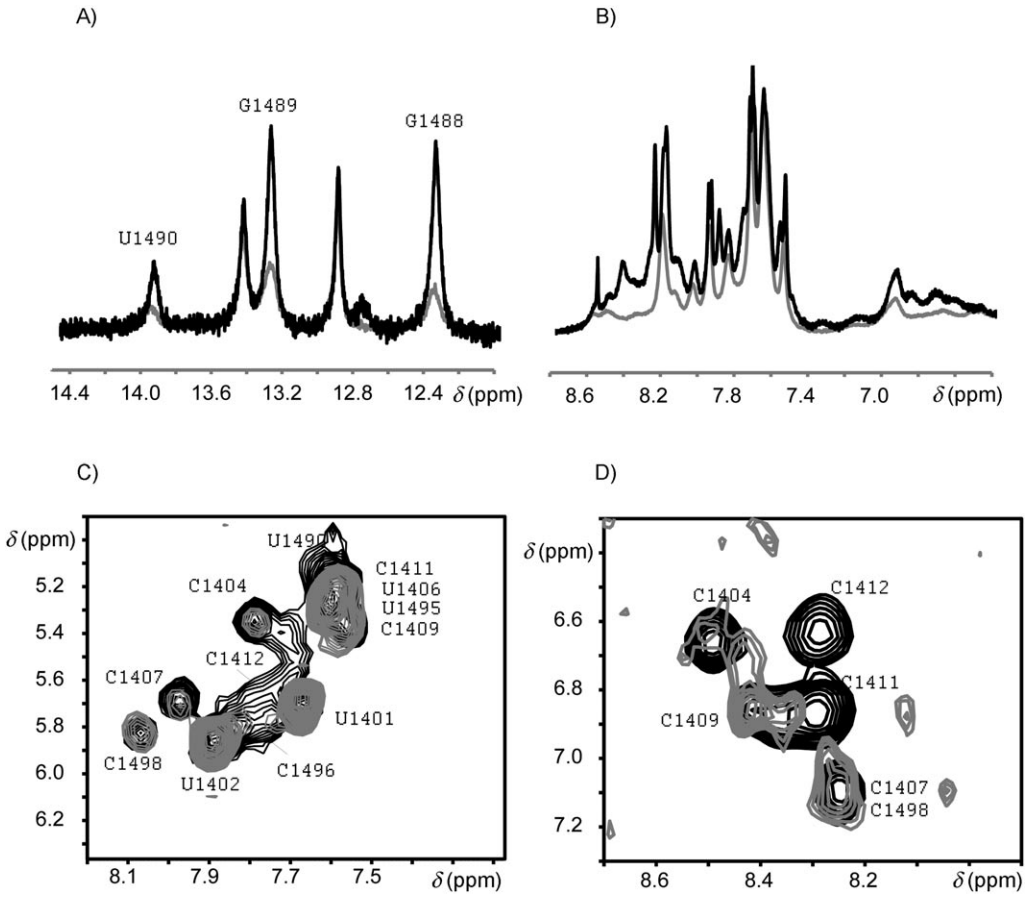

Figure 6. ^1H NMR spectra and 2D NOESY spectra of the RNA fragment (0.62 mM) in H_2O and phosphate buffer (20 mM) at pH 6.5 and $T = 298$ K in the absence of $Cu(NO_3)_2$ (black) and in the presence of $Cu(NO_3)_2$ in a $Cu(NO_3)_2$/RNA ratio of 1:5 (gray).

KanA. Addition of Cu^{II} ions to KanA under the experimental conditions used in the present study confirmed previous observations (Figure 7 A): an almost selective broadening of the signals for the hydrogen atoms on the C ring. Deeper insight into the broadening effect of copper(II) was provided by the TOCSY spectrum (not shown), which helps remove the severe overlap of the proton signals of different rings. Each sugar ring is a spin system for which all the proton signals are connected through *J* couplings. As there are no proton–proton *J* couplings between different rings, it is sufficient to find one isolated proton signal for a given ring to isolate one sugar spin system from the others. Figure 7 shows the disappearance of all correlations with 1″-H at the anomeric position of the C ring as a result of the broadening of its signal. Correlations that originate from 2″-H and 5″-H, the signals of which overlap, are still observable, and broadening is observed in their cross-peaks with 3″-H and 4"-H; less pronounced is the effect on 6"-H. Ring A is affected slightly, as shown by the correlations with the isolated anomeric hydrogen atom 1′-H. A small effect is observed in the cross-peak between 5′-H and the hydrogen atoms 6′-H. As for the B ring, the signals for the geminal hydrogen atoms 2-H are well isolated but intrinsically less intense, which makes the interpretation less straightforward; however, we can state that broadening is less severe and observed especially for 2-H_{ax} and 1-H. These results are in good agreement with previous observations: two or more complexes coexist in which coordination to the copper ion involves either the amine nitrogen atom of the C ring or both amine nitrogen atoms of the A and C rings. In the latter case, the copper ion is also brought into the proximity of the hydrogen atoms on the B ring.

Effect of copper on the RNA–KanA complex

To determine whether copper binds to KanA in its complex with RNA, we measured a NOESY spectrum of the antibiotic in the presence of both RNA (0.1 equiv) and Cu^{II} (0.1 equiv). As stated above, the NOESY cross-peaks originate only from the slowly tumbling bound form of the antibiotic. The disappearance of cross-peaks in the presence of Cu^{II} should in principle localize the paramagnetic ion. The comparison has to be made between the effect of Cu^{II} on the 1D ^{1}H NMR spectrum of the free antibiotic and the effect of Cu^{II} on the NOESY spectrum of the same sample in the presence of RNA. The use of the 1D spectrum to monitor the effects of Cu^{II} in the presence of a small amount of RNA would only give information about the free ligand, which is present in large excess. On the other hand, the NOESY spectrum of the free ligand can not be taken as a reference because of the inefficiency of the experiment with such medium-sized molecules (especially at 600 MHz). However, the linewidth of 2D peaks in the NOESY spectrum of the RNA-bound form of the antibiotic is still determined by the

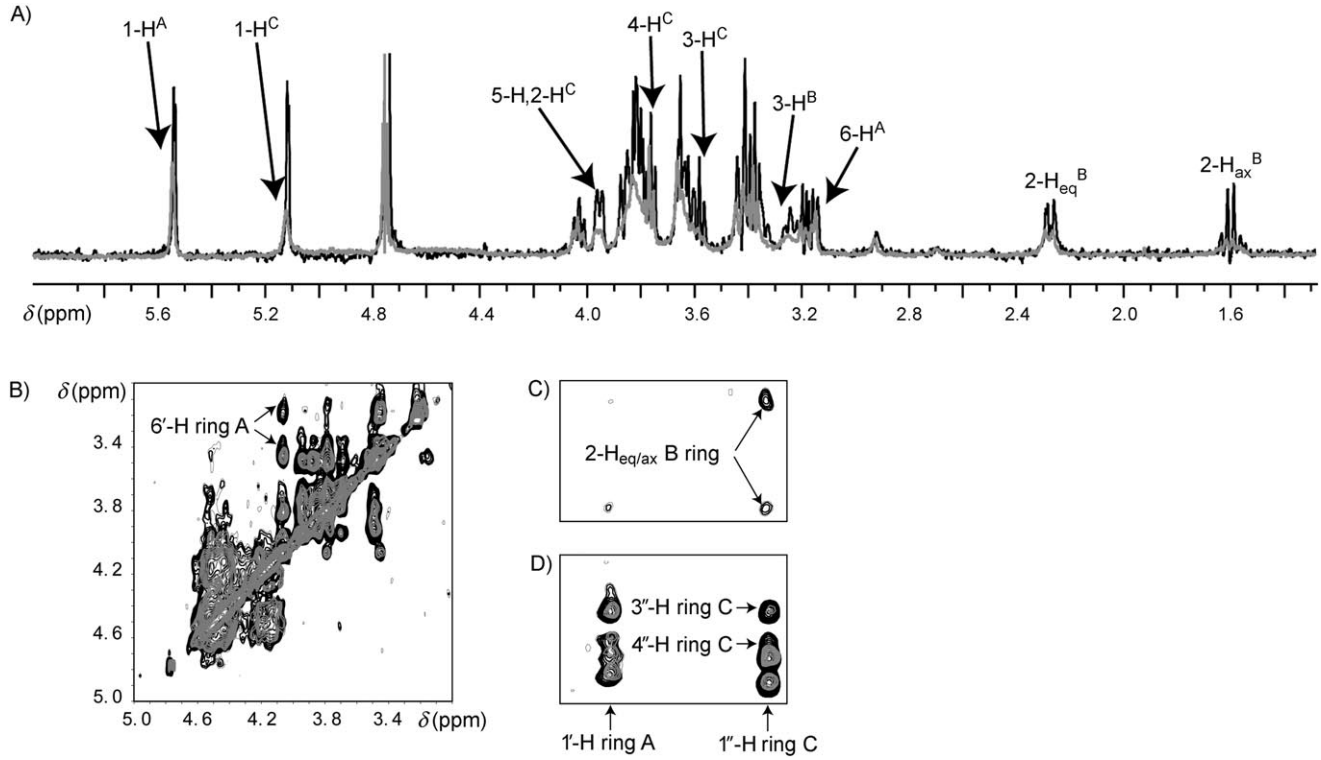

Figure 7. A) ^{1}H NMR spectra of kanamycin A (0.40 mM) in H_2O with phosphate buffer (20 mM) at pH 6.5 and $T = 298$ K in the absence of $Cu(NO_3)_2$ (black) and in the presence of $Cu(NO_3)_2$ in a $Cu(NO_3)_2$/KanA ratio of 1:10 (gray). Isolated resonances labeled A, B, or C, which refer to the rings of the antibiotic. B–D) 2D ^{1}H NOESY spectra of kanamycin A (0.40 mM) in H_2O with phosphate buffer (20 mM) at pH 6.5 and $T = 298$ K in the presence of the RNA fragment in an RNA/KanA ratio of 1:10. The spectra were recorded in the absence of $Cu(NO_3)_2$ (black) and in the presence of $Cu(NO_3)_2$ in a $Cu(NO_3)_2$/KanA ratio of 1:10 (gray). Correlations involving the 1-H-type hydrogen atoms on the A and C rings are shown in panels C and D.

transversal relaxation rate R_2; thus, there is a contribution from the free form of KanA. As data might be biased by the effect of copper on the free antibiotic, care must be taken in interpreting the data.

Regardless of these limitations, it is clear that copper(II) exerts different effects on kanamycin A in the absence and in the presence of RNA (Figure 7). The effect on the A ring is comparable to that on ring C (compare panels A and D in Figure 7). Overall, the effect of the Cu^{II} ion is strong, despite the competition from the many sites in the RNA molecule itself; this indicates the formation of a complex with some specificity. As the metal and the RNA are present in the same concentration, the observed differences show that the aminoglycoside antibiotic is a preferred ligand for copper coordination. The broadening of the proton signals for the 6′-H atoms in the A ring indicates binding to the amino group (Figure 7B). The effect on the C ring is still present, although diminished, and could in principle be ascribed to the contribution of the kanamycin A fraction not interacting with RNA. However, the relatively small broadening observed in the 1D NMR spectrum is not consistent with the near disappearance of NOESY correlations involving both 3′′-H and 4′′-H (Figure 7D). It is therefore likely that Cu^{II} binds to the amino group of this ring. Little can be said about the B ring, as broadening of the signals of the geminal hydrogen atoms 2-H was also observed in the absence of RNA (TOCSY spectrum, data not shown). All these observations indicate that the amino groups of the A and C rings (and possibly that of the B ring) are involved in the coordination of copper by kanamycin A bound to RNA. Paramagnetic effects can in principle originate from copper bound to RNA; however, the most important possible copper-binding sites on RNA (see the section "Effect of copper on RNA") are either far away from influenced kanamycin amino groups or so close to these groups as to suggest that copper-binding sites of the ternary kanamycin–Cu–RNA complex are involved.

Deeper insight into the possible features of the copper complex can be obtained by analyzing the X-ray crystal structure. If the observation that kanamycin A is bound "specifically" is taken into account, and our experimental evidence that copper binds to amino groups is considered, three possible sites are found. The first site would involve the amino and 4′′-hydroxy groups of ring C and N7 of G1405. This site was constructed by imposing copper coordination on these donors and adding one water molecule (as there are no other possible ligands, and a water molecule can be accommodated easily in the major groove). After energy minimization with the positions of all RNA and kanamycin atoms maintained, a distorted tetrahedron can be drawn with the geometrical parameters reported in Figure 8. Paramagnetic effects on RNA-bound KanA could also originate from the aspecific form. In this case, a similar copper site is still possible with the involvement of G1491.

The second site would involve one amino nitrogen atom of the B ring (at the 3-position) and N7 of G1494. Again, additional water was added, all atoms were left in the same position, and a complex with the geometrical parameters reported in Figure 8 was found. Most importantly, these sites involve two

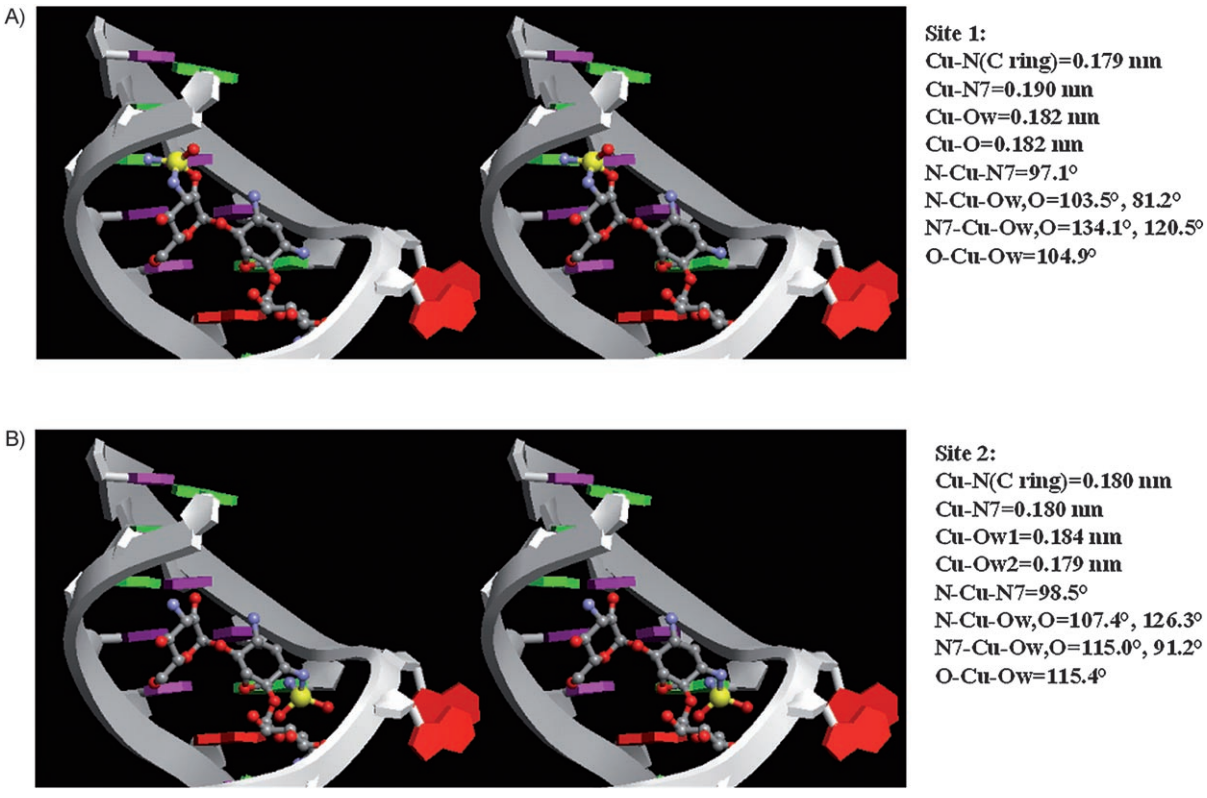

Figure 8. Geometrical parameters of two possible copper sites in the kanamycin–RNA complex. Guanine, adenine, and cytosine bases are represented in green, red, and violet, respectively. Copper is represented as a yellow sphere.

guanine residues that were indicated as targets for RNA degradation induced by copper.[54] Interestingly, this second site could be present in all crystal structures involving aminoglycoside antibiotics (such as paromomycin, meomycin B, lividomycin A), as the interaction between 3-N of the 2-deoxystreptamine ring (B ring) with N7 of G1494 is a conserved feature of the interaction of these antibiotics with the target RNA or DNA[47,55,56] and could indicate a common mechanism for enhanced antibacterial activity in the presence of copper.[30,45] However, in the aspecific form of KanA, ring B with its two amino groups is very exposed to the solvent, and the paramagnetic contributions observed could in principle also originate from copper bound to this form.

Finally, the amino group of the A ring could in principle bind with the N1 nitrogen atom of the adjacent residue A1408 or with N3 of C1409 for the specific form. Through motion of the branch that bears the amino group in ring A, G1491 could also become close. However, as this branch is generally involved in hydrogen bonding with the oxygen atom of the ring, its mobility is limited.[38] A further possible explanation for the paramagnetic effect observed at ring A is its vicinity to G–C pairs, which have been proposed as possible sites for the interaction of Cu^{II} with RNA.[57]

Conclusions

The NMR-based model that emerges from this study indicates that Cu^{II} ions could interact with the kanamycin–RNA complex by linking amino moieties of the antibiotic with N7 atoms of guanine bases. This finding suggests a possible role of the metal in the formation of 8-oxoguanine, a species often found as a product of nucleic acid degradation under conditions of oxidative stress.[54] The model would also explain the increased efficacy of antibiotics in the presence of copper.[30,45]

Experimental Section

The RNA oligonucleotide was synthesized by standard solid-state phosphoramidite chemistry on an Expedite 8909 Biosearch instrument by using Link Technologies phosphoramidites and was purified by reversed-phase and SAX (strong anion exchange) HPLC. The sample was heated at 95 °C for 5 min to promote annealing. The RNA sample was then dissolved to a concentration of 0.62 mM in H_2O or D_2O with phosphate buffer (20 mM) and NaCl (0.1 M), and the mixture was maintained at pH 6.5.

Kanamycin A sulfate was obtained from Fluka Chemie AG and dissolved to a concentration of 0.4 mM in D_2O with phosphate buffer (20 mM) and NaCl (0.1 M). The pH value of the sample was kept constant at 6.5.

Copper was added from a stock solution of $Cu(NO_3)_2$ to the KanA sample in a Cu^{II}/KanA ratio of 1:10, to the RNA sample in a Cu^{II}/RNA ratio of 1:5, and to the KanA–RNA complex in a KanA/RNA/Cu^{II} ratio of 10:1:1.

NMR spectroscopic experiments were carried out at 14.1 T on a Bruker Avance 600 spectrometer equipped with a Silicon Graphics workstation at a controlled temperature of ±0.1 K and with a TBI (triple broadband inverse) probe.

The proton resonances for the ligand and complexes were assigned by COSY, TOCSY, and NOESY experiments. The MLEV-17 pulse sequence, with a mixing time of 90 ms, was used for the TOCSY experiments. NOESY spectra were acquired with a mixing time of 400 ms. All experiments were processed on a Silicon Graphics O2 workstation by using XWINNMR 2.6 software.

The intensities of NOESY cross-peaks of KanA in the presence of RNA were converted into intramolecular proton–proton distance restraints, which were used to construct a pseudo potential energy for the calculation of restrained simulated annealing (SA) in torsional angle space to obtain the structure of KanA when bound to the RNA A site. We performed the calculation with the program DYANA[53] by using 10000 steps and 300 random starting conformers of KanA. Distance restraints were determined by referencing peak volumes to cross-peaks corresponding to proton pairs at fixed distances within a single ring. To take into account possible differences in the mobility of each ring, we calibrated the peaks for ring A on the basis of the proton pair 1′-H–2′-H and the peaks for ring C on the basis of 1‴-H–4‴-H. The error in calculated distances was estimated by evaluating the noise in the NOESY spectrum. Proton pairs for which no NOESY cross-peak was observed were assigned a lower distance limit of 0.5 nm.

Energy minimizations of the KanA–Cu–RNA complex were performed in vacuo with the program Hyperchem.[58] The MM+ force field was used, and the copper(II) ion was positioned in either of the two hypothesized binding sites. Coordination of the copper(II) ion was imposed on appropriate donors, and a number of water molecules were added to complete the coordination sphere of four donors.

Acknowledgements

We acknowledge the MIUR (FIRB RBNE03PX83_003) and the C.I.R.M.M.P. (Consorzio Interuniversitario Risonanze Magnetiche di Metalloproteine Paramagnetiche) for financial support.

Keywords: aminoglycosides · copper · NMR spectroscopy · ribosomal A site · RNA

[1] S. Magnet, J. S. Blanchard, *Chem. Rev.* **2005**, *105*, 477–498.
[2] M.-P. Mingeot-Leclercq, Y. Glupczynski, P. M. Tulkens, *Antimicrob. Agents Chemother.* **1999**, *43*, 727–737.
[3] L. P. Kotra, J. Haddod, S. Mobashery, *Antimicrob. Agents Chemother.* **2000**, *44*, 3249–3256.
[4] T. Hermann, E. Westhof, *Comb. Chem. High Throughput Screening* **2000**, *3*, 219–234.
[5] Q. Vicens, E. Westhof, *ChemBioChem* **2003**, *4*, 1018–1023.
[6] D. Moazed, H. F. Noller, *Nature* **1987**, *327*, 389–394.
[7] J. M. Ogle, D. E. Brodersen, W. M. Clemons, M. J. Tarry, A. P. Carter, V. Ramakrishnan, *Science* **2001**, *292*, 897–902.
[8] B. T. Wimberly, D. E. Brodersen, W. M. Clemons, R. J. Morgan-Warren, A. P. Carter, C. Vonrhein, T. Hartsch, V. Ramakrishnan, *Nature* **2000**, *407*, 327–339.
[9] J. M. Ogle, F. V. Murphy, M. J. Tarry, V. Ramakrishnan, *Cell* **2002**, *111*, 721–732.
[10] J. M. Ogle, A. P. Carter, V. Ramakrishnan, *Trends Biochem. Sci.* **2003**, *28*, 259–266.
[11] J. Davies, L. Gorini, B. D. Davis, *Mol. Pharmacol.* **1965**, *1*, 93–106.
[12] J. Davies, B. D. Davis, *J. Biol. Chem.* **1968**, *243*, 3312–3316.
[13] B. D. Davis, *Microbiol. Rev.* **1987**, *51*, 341–350.
[14] C. M. Spahn, C. D. Prescott, *J. Mol. Med.* **1996**, *74*, 423–439.
[15] A. P. Carter, W. M. Clemons, D. E. Brodersen, R. J. Morgan-Warren, B. T. Wimberly, V. Ramakrishnan, *Nature* **2000**, *407*, 340–348.

[16] A. Forge, J. Schacht, *Audiol. Neuro-Otol.* **2000**, *5*, 3–22.
[17] W. E. Siegenthaler, A. Bonetti, R. Luthy, *Am. J. Med.* **1986**, *80*, 2–14.
[18] P. Sinswat, W.-J. Wu, S.-H. Sha, J. Schacht, *Kidney Int.* **2000**, *58*, 2525–2532.
[19] L. S. Gonzalez III, J. P. Spencer, *Am. Fam. Physician* **1998**, *58*, 1811–1820.
[20] P. M. Tulkens, *Toxicol. Lett.* **1989**, *46*, 107–123.
[21] B. H. Ali, A. K. Bashir, I. T. Mugamer, M. O. Tanira, *Hum. Exp. Toxicol.* **1996**, *15*, 51–55.
[22] E. M. Priuska, K. Clark-Baldwin, V. L. Pecoraro, J. Schacht, *Inorg. Chim. Acta* **1998**, *273*, 85–91, and references therein.
[23] F. Freire, I. Cuesta, F. Corzana, J. Revuelta, C. González, M. Hricovini, A. Bastida, J. Jiménez-Barbero, J. L. Asensio, *Chem. Commun.* **2007**, 174–176.
[24] S. Steenken, S. V. Jovanovic, *J. Am. Chem. Soc.* **1997**, *119*, 617–618.
[25] A. Patwardhan, J. A. Cowan, *Chem. Commun. (Camb. UK)* **2001**, 1490–1491.
[26] C. A. Chen, J. A. Cowan, *Chem. Commun. (Camb. UK)* **2002**, 196–197.
[27] M. Jezowska-Bojczuk, W. Lesniak, W. Bal, H. Kozłowski, K. Gatner, A. Jezierski, J. Sobczak, S. Mangani, W. Meyer-Klaucke, *Chem. Res. Toxicol.* **2001**, *14*, 1353–1362.
[28] L. H. Guo, H. A. Hill, D. J. Hopper, G. A. Lawrance, G. S. Sanghera, *J. Biol. Chem.* **1990**, *265*, 1958–1963.
[29] W. Szczepanik, P. Kaczmarek, J. Sobczak, W. Bal, K. Gatner, M. Jeżowska-Bojczuk, *New J. Chem.* **2002**, *26*, 1507–1514.
[30] A. Sreedhara, A. Patwardhan, J. A. Cowan, *Chem. Commun.* **1999**, 1147–1148.
[31] M. Jezowska-Bojczuk, W. Bal, H. Kozłowski, *Inorg. Chim. Acta* **1998**, *275–276*, 541–545.
[32] M. Jezowska-Bojczuk, W. Bal, *J. Chem. Soc. Dalton Trans.* **1998**, 153–159.
[33] T. D. Rae, P. J. Schmidt, R. A. Pufahl, V. C. Culotta, T. V. O'Halloran, *Science* **1999**, *284*, 805–808.
[34] T. Theophanides, J. Anastassopoulou, *Crit. Rev. Oncol./Hematol.* **2002**, *42*, 57–64.
[35] D. Bar-Or, L. T. Rael, E. P. Lau, N. K. Rao, G. W. Thomas, J. V. Winkler, R. L. Yukl, R. G. Kingston, C. G. Curtis, *Biochem. Biophys. Res. Commun.* **2001**, *284*, 856–862.
[36] M. C. Linder, *Biochemistry of Copper*, Plenum, New York, **1991**.
[37] W. Szczepanik, A. Czarny, E. Zaczynska, M. Jeżowska-Bojczuk, *J. Inorg. Biochem.* **2004**, *98*, 245–253.
[38] N. D'Amelio, E. Gaggelli, N. Gaggelli, E. Molteni, M. C. Baratto, G. Valensin, M. Jeżowska-Bojczuk, W. Szczepanik, *Dalton Trans.* **2004**, 363–368.
[39] X. Lu, M. Zhang, J. Kang, X. Wang, L. Zhuo, H. Liu, *J. Inorg. Biochem.* **2004**, *98*, 582–588.
[40] M. Jezowska-Bojczuk, W. Bal, K. S. Kasprzak, *J. Inorg. Biochem.* **1996**, *64*, 231–246.
[41] M. Jezowska-Bojczuk, W. Szczepanik, W. Lesniak, J. Ciesiolka, J. Wrzesinski, W. Bal, *Eur. J. Biochem.* **2002**, *269*, 5547–5556.
[42] A. Sreedhara, J. A. Cowan, *Chem. Commun.* **1998**, 1737–1738.
[43] W. Szczepanik, P. Kaczmarek, M. Jeżowska-Bojczuk, *Bioinorg. Chem. Appl.* **2004**, *2*, 55–68.
[44] S. Dhar, M. Nethaji, A. R. Chakravarty, *Dalton Trans.* **2004**, 4180–4184.
[45] A. Sreedhara, J. A. Cowan, *J. Biol. Inorg. Chem.* **2001**, *6*, 166–172.
[46] W. Szczepanik, E. Dworniczek, J. Ciesiołka, J. Wrzesinski, J. Skała, M. Jeżowska-Bojczuk, *J. Inorg. Biochem.* **2003**, *94*, 355–364.
[47] B. François, R. J. M. Russell, J. B. Murray, F. Aboul-ela, B. Masquida, Q. Vicens, E. Westhof, *Nucleic Acids Res.* **2005**, *33*, 5677–5690.
[48] S. R. Lynch, R. L. Gonzalez, J. D. Puglisi, *Structure* **2003**, *11*, 43–53.
[49] F. Corzana, I. Cuesta, F. Freire, J. Revuelta, M. Torrado, A. Bastida, J. Jiménez-Barbero, J. L. Asensio, *J. Am. Chem. Soc.* **2007**, *129*, 2849–2865.
[50] N. D'Amelio, E. Gaggelli, N. Gaggelli, F. Mancini, E. Molteni, D. Valensin, G. Valensin, *J. Inorg. Biochem.* **2003**, *95*, 225–229.
[51] J. Reuben, *J. Am. Chem. Soc.* **1973**, *95*, 3534–3540.
[52] C. H. Wong, M. Hendrix, E. S. Priestley, W. A. Greenberg, *Chem. Biol.* **1998**, *5*, 397–406.
[53] P. Güntert, C. Mumenthaler, K. Wüthrich, *J. Mol. Biol.* **1997**, *273*, 283–298.
[54] O. I. Aruoma, B. Halliwell, E. Gajewski, M. Dizdaroglu, *Biochem. J.* **1991**, *273*, 601–604.
[55] Q. Vicens, E. Westhof, *J. Mol. Biol.* **2003**, *326*, 1175–1188.
[56] S. Yoshizawa, D. Fourmy, R. G. Eason, J. D. Puglisi, *Biochemistry* **2002**, *41*, 6263–6270.
[57] R. K. O. Sigel, A. Vaidya, A. M. Pyle, *Nature Struct. Biol.* **2000**, *7*, 1111–1116.
[58] HYPERCHEM, Release 5.1 Pro for Windows, Hypercube Inc., Waterloo, ON, **1997**.

Received: July 13, 2007
Published online on November 30, 2007

